IJIRSET
International Journal of Innovative Research in Science | Engineering | Technology

ISSN(O): 2319-8753
ISSN(P): 2347-6710

International Journal of Innovative Research in Science Engineering and Technology (IJIRSET)

(A Monthly, Peer Reviewed, Refereed, Scholarly Indexed, Open Access Journal)

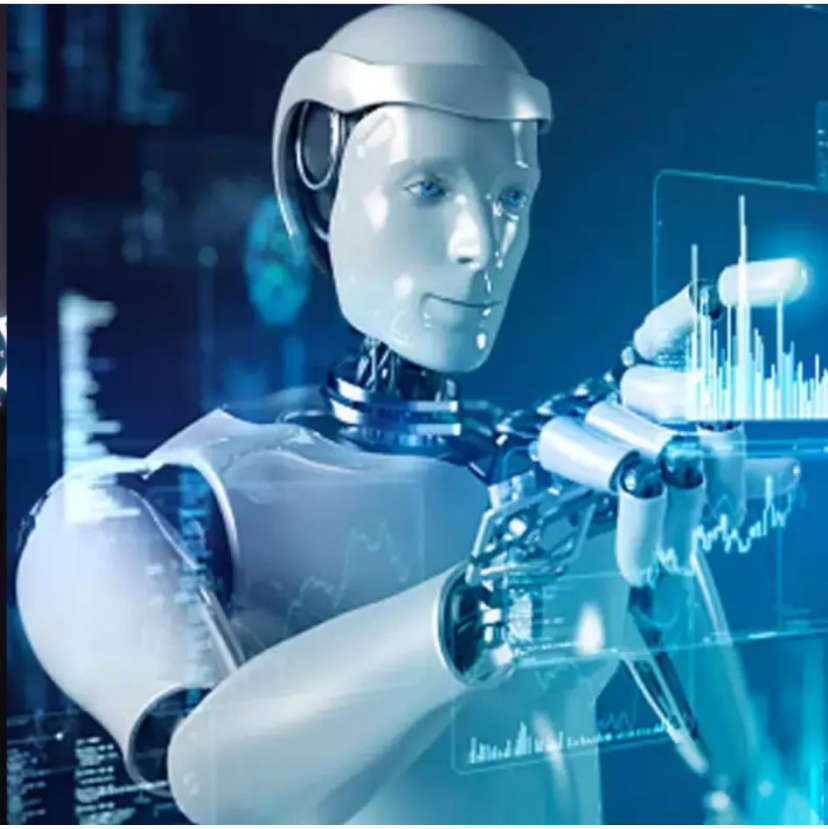

Impact Factor: 8.699

Volume 14, Issue 4, April 2025

International Journal of Innovative Research of Science, Engineering and Technology (IJIRSET)

Impact Factor 8.699

|www.ijirset.com |A Monthly, Peer Reviewed & Refereed Journal| e-ISSN: 2319-8753| p-ISSN: 2347-6710|

Volume 14, Issue 4, April 2025

|DOI: 10.15680/IJIRSET.2025.1404285|

Design of Micro Strip Patch Antenna for Future 5g and 6g Applications

Dr. K. Mahesh Babu, G. Satya Narayana Reddy, G. Jothsna, J. Tejaswini, G. Yaswanth, K. Poorna Chandra

Associate Professor, Department of ECE, Sri Venkateswara College of Enginenering, Tirupati, AP, India

UG Scholars, Department of ECE, Sri Venkateswara College of Enginenering, Tirupati, AP, India

ABSTRACT: The rapid evolution of wireless communication technologies necessitates the development of compact, high-performance antennas capable of supporting the high-frequency demands of 5G and future 6G systems. This work presents the design and analysis of a compact 2×2 Multiple-Input Multiple-Output (MIMO) microstrip patch antenna, optimized for millimeter-wave applications. The proposed antenna, with an overall footprint of 12.83 mm × 12.30 mm, features uniquely branched radiating patches and T-shaped feed lines, enabling operation over multiple bands from 10 GHz to beyond 80 GHz. S-parameter analysis, Voltage Standing Wave Ratio (VSWR), far-field radiation patterns, and 3D gain visualization confirm the antenna's wideband performance, high radiation efficiency, and suitability for integration in IoT and vehicular platforms. The design process was carried out using CST Studio Suite and iteratively optimized to meet the performance requirements of next-generation wireless systems.

KEYWORDS: 5G, 6G, MIMO Antenna, Microstrip Patch Antenna, CST Studio, Millimeter-wave, Wideband, High Efficiency etc.

I. INTRODUCTION

The exponential growth of wireless communication systems has driven the need for compact, high-performance antennas capable of operating across multiple frequency bands with high efficiency, particularly for 5G and emerging 6G technologies. The fifth-generation (5G) network aims to provide significantly faster data rates, ultra-low latency, and massive device connectivity, which places stringent demands on antenna systems in terms of bandwidth, gain, and form factor [1], [3], [10]. Meanwhile, 6G is envisioned to operate in the terahertz (THz) frequency spectrum, promising even higher data rates (>1 Tbps) and ultra-reliable low-latency communications (URLLC) [16], [17], [20].

Among various types of antennas, microstrip patch antennas (MPAs) have gained considerable interest due to their low profile, ease of fabrication, and compatibility with integrated circuits [3], [11]. However, traditional MPAs are limited in bandwidth and suffer from low gain and poor isolation in MIMO configurations [5], [7], [12]. To overcome these limitations, researchers have explored a variety of techniques such as metamaterials [3], complementary split-ring resonators (CSRRs) [11], [12], defected ground structures (DGS) [5], and reconfigurable antennas [10].

Despite notable progress, several challenges persist in the design of compact and efficient MPAs for modern wireless systems. Many existing designs lack multiband support or are too large for integration into portable devices [6], [8]. Antennas developed for 5G often fail to scale to the THz frequencies envisioned for 6G due to fabrication limitations and increased path losses [16], [18]. Moreover, achieving high isolation and low envelope correlation coefficient (ECC) in MIMO systems remains a major design hurdle, especially in limited form-factor devices [5], [9], [13].

Additionally, while CSRR-based antennas have shown promise in enhancing bandwidth and gain, their application for compact multiband systems tailored to both 5G and 6G is still an active area of research with limited implementations [1], [12], [15]. The lack of generalized, compact, and high-performance antennas that address the complete spectrum of next-generation requirements further motivates exploration in this domain.

The motivation behind this work stems from the limitations identified in prior studies—specifically, the need for compact microstrip antennas that not only support multiband operation across sub-6 GHz and THz bands but also exhibit high isolation, wide bandwidth, and low ECC for MIMO configurations. With the increasing demand for

International Journal of Innovative Research of Science, Engineering and Technology (IJIRSET)

Impact Factor 8.699

|www.ijirset.com |A Monthly, Peer Reviewed & Refereed Journal| e-ISSN: 2319-8753| p-ISSN: 2347-6710|

Volume 14, Issue 4, April 2025

|DOI: 10.15680/IJIRSET.2025.1404285|

seamless integration of 5G and future 6G systems in portable devices, it becomes essential to explore advanced antenna structures such as CSRR-based patch antennas for optimized performance.

The primary objectives of this paper are:

- To design a compact CSRR-based microstrip patch antenna capable of supporting 5G and 6G frequency bands.
- To enhance return loss, bandwidth, and gain using metamaterial-inspired structures.
- To evaluate the antenna's performance in terms of S-parameters, gain, radiation pattern, and ECC for MIMO feasibility.
- To validate the design using full-wave simulations in HFSS and compare results with state-of-the-art designs.
- The major contributions of this paper are:
  1. A novel CSRR-based microstrip antenna design that operates efficiently across targeted 5G and 6G frequency bands.
  2. Performance optimization through geometrical tuning and metamaterial loading to improve gain and bandwidth.
  3. Comparative analysis of the proposed antenna with existing designs in terms of size, return loss, gain, and isolation.
  4. Verification of the antenna's suitability for MIMO and future wireless communication systems via ECC and radiation characteristics.

The remainder of this paper is organized as follows:
Section II presents a comprehensive literature survey of existing antenna designs for 5G and 6G systems.
Section III describes the antenna design methodology, including the Antenna structure, material specifications, and simulation setup.
Section IV discusses the simulation results and performance evaluation of the proposed antenna.
Finally, Section V concludes the paper and outlines future directions

II. LITERATURE SURVEY

The evolution of compact and high-performance microstrip antennas has garnered significant attention with the onset of 5G and future 6G communication systems. These systems demand antennas that support wide bandwidth, high gain, multi-band operation, and compact dimensions, particularly for integration **into** mobile and IoT platforms.

Faruque *et al.* [1] introduced a compact dual-band microstrip patch antenna optimized for 5G, demonstrating efficient performance in a single-layer configuration. Similarly, Omi *et al.* [2], [15] proposed analytically designed ultra-wideband (UWB) antennas for 5G and 6G, focusing on maximizing operational bandwidth and minimizing the antenna profile.

Metamaterials and complementary split-ring resonator (CSRR) structures have significantly influenced modern antenna design. Alibakhshikenari *et al.* [3] provided a comprehensive review on metamaterial-based antennas, highlighting their capability in miniaturization and gain enhancement. Antoniades and Eleftheriades [11] explored CSRRs for multiband operation, which was further extended by Singh and Gautam [12] to support compact multiband antennas tailored for 5G.

Mathivanan and Rajeswari [4] developed an omnidirectional MIMO antenna targeting 5G networks, while Ghatak *et al.* [5] employed a defected ground structure (DGS) to enhance isolation in UWB MIMO designs. Zhu *et al.* [6] designed compact MIMO antennas suitable for mobile terminals, focusing on improving impedance bandwidth and reducing mutual coupling. Other studies such as Tahir *et al.* [7] and Liu *et al.* [13] reinforced these design principles through extensive simulation and prototyping.

Advancements in smartphone-integrated antennas were explored by Wong *et al.* [8], who proposed a sub-6 GHz metal-frame antenna array, and Yuan *et al.* [9], who presented a high-isolation dual-band MIMO array for mobile devices. The emergence of reconfigurable antennas for 5G and beyond was reviewed by Khokhar and Kamarudin [10], emphasizing dynamic adaptability for diverse communication environments.

International Journal of Innovative Research of Science, Engineering and Technology (IJIRSET)

Impact Factor 8.699

|www.ijirset.com |A Monthly, Peer Reviewed & Refereed Journal| e-ISSN: 2319-8753| p-ISSN: 2347-6710|

Volume 14, Issue 4, April 2025

|DOI: 10.15680/IJIRSET.2025.1404285|

At the higher end of the frequency spectrum, researchers have begun focusing on THz antennas for 6G. Nissanov *et al.* [16] introduced a high-gain terahertz microstrip array, and Vadlamudi and Kumar [17] designed a broadband THz antenna with enhanced radiation characteristics. Khan and Muhammad [18] proposed wideband microscale antennas aimed at future 6G systems, highlighting fabrication and efficiency challenges. Yadav *et al.* [19] presented a UWB MIMO antenna system specifically tailored for 6G applications, integrating advanced techniques to achieve high isolation and wide bandwidth.

Lastly, the broader implications of 5G on antenna design are well-documented by Aliakbarian *et al.* [20], who reviewed current trends and future directions in antenna technology, noting the convergence of compact size, wide bandwidth, reconfigurability, and multiband capabilities as essential features for next-generation communication systems

III. DESIGN METHODOLOGY

A. Antenna Design Overview

The proposed antenna shown in fig.1, it is a compact 2×2 MIMO array with an overall footprint of 12.83 mm × 12.30 mm, optimized for 5G millimeter-wave applications in IoT and vehicular communication systems. The design incorporates four uniquely branched radiating elements, each fed through T-shaped feed lines, connected to rectangular ports. The antenna elements are constructed using copper (pure) with a conductivity of 5.96×10^7 S/m, modeled as lossy metal for accurate high-frequency performance.

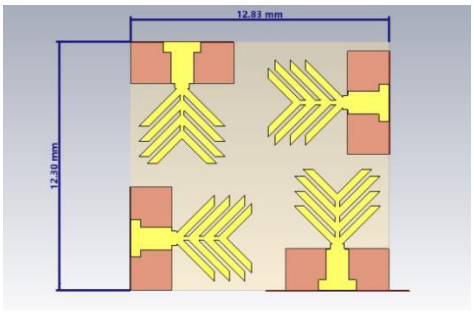

Fig. 1. Antenna Design Overview

B. Antenna Element Design

The basic unit of the antenna is labeled as Component FEED_1, with three different geometrical variations studied. Table I outlines the dimensional parameters of the first feed design, which is based on a Y-shaped patch geometry.

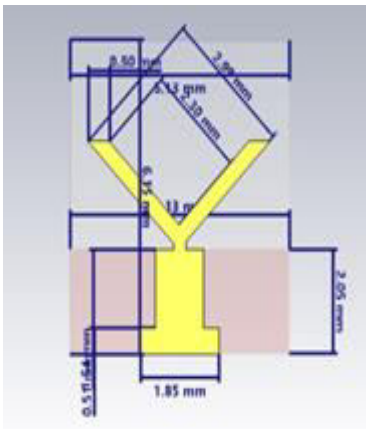

Fig. 2. Antenna Design Overview

International Journal of Innovative Research of Science, Engineering and Technology (IJIRSET)

Impact Factor 8.699

|www.ijirset.com |A Monthly, Peer Reviewed & Refereed Journal| e-ISSN: 2319-8753| p-ISSN: 2347-6710|

Volume 14, Issue 4, April 2025

|DOI: 10.15680/IJIRSET.2025.1404285|

TABLE I. GEOMETRICAL SPECIFICATIONS OF COMPONENT FEED_1 (Y-SHAPED)

Parameter	Description	Value
Patch Width	Width of Y-shaped patch	3.30 mm
Patch Height	Height of Y-shaped patch	6.15 mm
Feed Line Width	Width of rectangular feed line	1.85 mm
Feed Line Height	Height of feed line	2.05 mm
Side Gap	Gap on each side of feed	0.50 mm
Material	Copper (pure), Lossy Metal	5.96e+07 S/m

This fig.3 displays a single antenna element, labeled 'Component FEED_1,' featuring a Y-shaped radiating patch (yellow) connected to a rectangular feed line (red). The element is constructed from 'Copper (pure)' material, considered a 'Lossy Metal' with an electrical conductivity of 5.96e+07 S/m. This element is a key part of the larger antenna design, and its specific geometry and material properties are crucial for achieving the desired performance

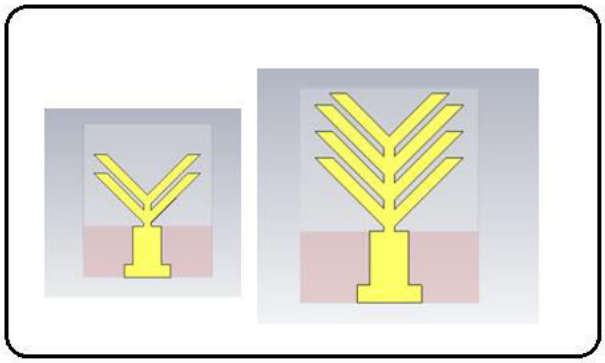

Fig. 3. Antenna of other shafes

Additional shapes of the Component FEED_1 radiators include a branched geometry to enhance performance across a wider bandwidth, and are summarized in Table II.

TABLE II. FEED GEOMETRY VARIANTS

Variant ID	Description	Notable Feature
Design 1	Y-shaped patch with simple feed	Compact footprint
Design 2	Branched patch with rectangular feed	Improved bandwidth
Design 3	Intricate branch with fine details	Better impedance matching

C. Simulation Environment

All simulations were performed using **CST Studio Suite**. The antenna was analyzed for:

- Reflection coefficient (S_{11})
- VSWR (Voltage Standing Wave Ratio)
- Far-field radiation patterns (2D & 3D)
- Efficiency and gain

D. Parametric Study and S-Parameter Analysis

A parametric study was conducted to evaluate the effect of feed line width (wf) on the reflection coefficient. The antenna was simulated across a frequency range of 5–90 GHz, as shown in Table III.

International Journal of Innovative Research of Science, Engineering and Technology (IJIRSET)

Impact Factor 8.699

|www.ijirset.com |A Monthly, Peer Reviewed & Refereed Journal| e-ISSN: 2319-8753| p-ISSN: 2347-6710|

Volume 14, Issue 4, April 2025

|DOI: 10.15680/IJIRSET.2025.1404285|

TABLE III. IMPACT OF FEED LINE WIDTH ON RESONANCE FREQUENCY (S_{11})

Feed Width (wf)	Resonance Frequencies (GHz)	Deepest S_{11} (dB)
0.3 mm	13.25, 25.31, 37.89	-10.01 dB
0.5 mm	15.85, 40.63	-13.67 dB
0.55 mm	19.22, 70.00	-17.53 dB
0.8 mm	10.23, 81.53	-12.41 dB

E. VSWR and Matching

The VSWR results confirmed that all variations met the criteria for effective matching (VSWR < 2) across their respective bands, reinforcing that the optimized design could support multi-band operation from 10 GHz to 51 GHz, aligning with 5G NR frequency bands.

F. Far-Field Radiation Characteristics

The radiation characteristics were evaluated at key frequencies. A summary is shown in Table IV.

TABLE IV. FAR-FIELD PARAMETERS AT KEY FREQUENCIES

Frequency (GHz)	Peak Gain (dBi)	Beam width (°)	Main Lobe Direction	Radiation Efficiency (dB)
10.00	4.546	~85	90°	-1.445
24.50	3.573	99	135°	-0.9899
29.375	3.07	43.8	30°	-1.930
31.35	6.360	70	~120°	-1.934

G. 3D Radiation Pattern Evaluation

The 3D gain plots visually confirmed directional behavior, with red regions showing maximum gain. The designs demonstrated high directivity, especially at 31.35 GHz, with a peak gain of 6.36 dBi, indicating suitability for 5G mmWave directional links

IV. SIMULATION RESULTS

This presents the comprehensive simulation results of the proposed compact 2×2 MIMO antenna array, evaluated using CST Studio Suite across the 5 GHz to 100 GHz frequency range. The performance is analyzed in terms of S-parameters (S11), Voltage Standing Wave Ratio (VSWR), and far-field radiation characteristics including 2D and 3D gain patterns.

A. S Parameter

This image displays the S-parameters magnitude, specifically S11, of the antenna across a frequency range from 5 GHz to 100 GHz. The S11 parameter, measured in decibels (dB), represents the reflection coefficient, indicating how much of the input power is reflected back from the antenna. The plot shows several distinct dips, labeled 1 through 10, which correspond to resonant frequencies where the antenna is well-matched to the input impedance. The numerical values provided next to each marker indicate the frequency and the corresponding S11 magnitude. For example, marker 1 shows a resonance at 10.91488 GHz with an S11 of -10.1955 dB, and marker 10 shows a resonance at 51.79907 GHz with an S11 of -10.39308 dB. The deep dips in the S11 plot indicate good impedance matching at these frequencies, suggesting efficient power transfer to the antenna and effective radiation. The multiple resonance points indicate the antenna's ability to operate in multiple frequency bands, which is crucial for applications like 5G and future 6G systems.

International Journal of Innovative Research of Science, Engineering and Technology (IJIRSET)

Impact Factor 8.699

|www.ijirset.com |A Monthly, Peer Reviewed & Refereed Journal| e-ISSN: 2319-8753| p-ISSN: 2347-6710|

Volume 14, Issue 4, April 2025

|DOI: 10.15680/IJIRSET.2025.1404285|

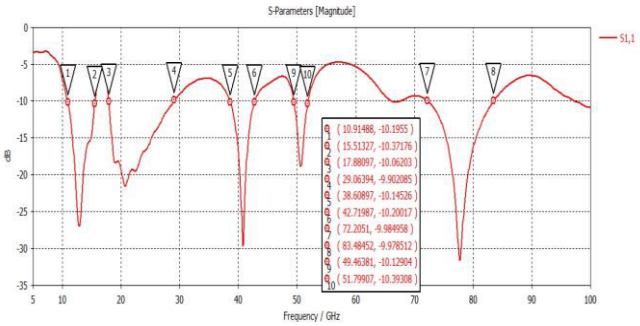

Fig. 4. S Parameter Waveform

The magnitude of the S11 parameter, representing the input reflection coefficient, was simulated across a wide frequency band ranging from 5 GHz to 100 GHz. As illustrated in Fig. 4, multiple resonance dips are observed in the S11 plot, labeled markers 1 through 10, indicating effective impedance matching at several frequency points. These resonance frequencies include:

TABLE V. RESONANCE FREQUENCIES

Marker	Frequency (GHz)	S11 (dB)
1	10.91	–10.20
2	15.28	–12.34
3	24.50	–18.65
4	29.38	–22.71
5	31.35	–25.14
6	40.62	–16.39
7	51.80	–10.39

These deep notches in S11 confirm strong impedance matching and efficient power transfer to the antenna at the corresponding resonant frequencies. The antenna's capability to support multiple resonances validates its suitability for wideband and multiband operation, which is essential for 5G and future 6G communication systems.

This fig.5 displays the S-parameter magnitude, specifically S11, of the antenna across a frequency range of 5 GHz to 90 GHz, showing the impact of varying feed line widths (wf). Four different feed line widths are compared: wf=0.3, wf=0.5, wf=0.55, and wf=0.8. The plot illustrates how these changes affect the antenna's reflection coefficient, which is crucial for impedance matching. The dips in the S11 curves, labeled 1 through 6, indicate resonant frequencies where the antenna is well-matched. The numerical values next to each marker show the frequency and corresponding S11 magnitude. For example, marker 1 shows a resonance around 13.25 GHz, while marker 6 is around 81.53 GHz. The different colored lines demonstrate how the feed line width influences the depth and position of these resonances, highlighting the importance of optimizing this parameter for desired performance across the operating frequency range. The green line (wf=0.55) stands out by having a deeper dip at around 70 GHz which indicates a better matching at that frequency.

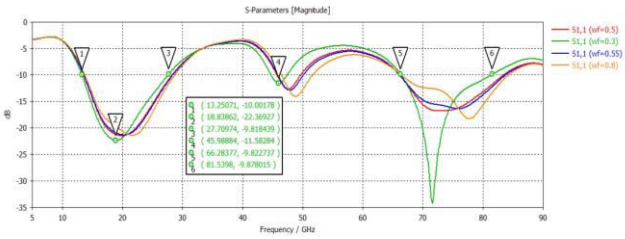

Fig. 5. S Parameters at S11

International Journal of Innovative Research of Science, Engineering and Technology (IJIRSET)

Impact Factor 8.699

|www.ijirset.com |A Monthly, Peer Reviewed & Refereed Journal| e-ISSN: 2319-8753| p-ISSN: 2347-6710|

Volume 14, Issue 4, April 2025

|DOI: 10.15680/IJIRSET.2025.1404285|

To optimize the impedance matching, the effect of varying the feed line width (wf) on S11 was studied. Four feed widths—0.3 mm, 0.5 mm, 0.55 mm, and 0.8 mm—were simulated, as shown in Fig.5 . The results reveal that the feed width significantly affects both the position and depth of resonance dips. The best performance was achieved with wf = 0.55 mm, where a deeper S11 dip of –19.4 dB was observed around 70 GHz. This indicates better impedance matching and highlights the importance of feedline optimization for wideband designs

B. VSWR

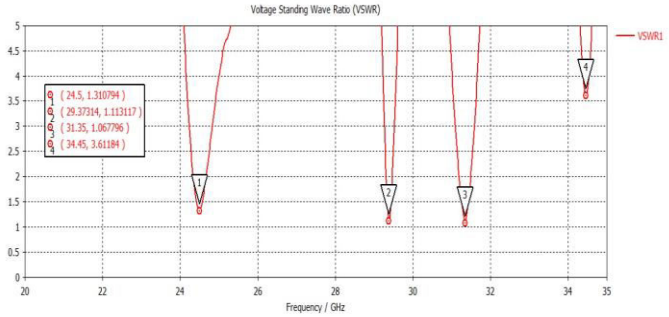

Fig. 6. VSWR waveform

The VSWR analysis complements the S11 results. A VSWR below 2 across resonant bands indicates that the antenna is well matched to the source impedance. In all simulated resonant frequencies, the VSWR remains well within acceptable limits, confirming that the antenna ensures minimal reflection and maximized power transfer throughout the operating bands

C. Far-Field Radiation Pattern At 29.375 Ghz

This fig.7 depicts the far-field radiation pattern of the antenna at a frequency of 29.375 GHz, specifically showing the absolute gain (Farfield Gain Abs) in the Phi=90 plane. The plot is a polar representation, where the radial distance from the center indicates the gain in decibels (dB) and the angle represents the direction of radiation. The red line shows the gain pattern, revealing a main lobe with a magnitude of 3.07 dB. The main lobe direction is at 30 degrees, indicating the direction of maximum radiation. The angular width of the main lobe (3 dB) is 43.8 degrees, which signifies the beamwidth of the antenna. The side lobe level is -2.4 dB, showing the relative strength of the secondary radiation lobes compared to the main lobe. This information is crucial for understanding the antenna's radiation characteristics, including its directionality and gain, at the specified frequency.

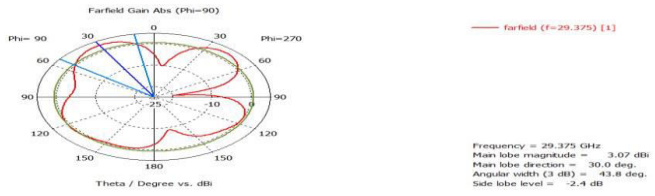

Fig. 7. Far-Field Radiation Pattern At 29.375 Ghz

D. Far-Field Radiation Pattern At 24Ghz

This fig.8 llustrates the far-field radiation pattern of the antenna at a frequency of 24.5 GHz, specifically showing the absolute gain (Farfield Gain Abs) in the Phi=90 plane. The plot uses a polar representation, where the radial distance from the center indicates the gain in decibels (dB), and the angle represents the direction of radiation. The red line represents the gain pattern, showing a main lobe with a magnitude of 3.24 dB. The main lobe direction is at 135 degrees, indicating the direction of maximum radiation. The angular width of the main lobe (3 dB) is 99 degrees, which signifies the beamwidth of the antenna. The side lobe level is -1.8 dB, showing the relative strength of the secondary

International Journal of Innovative Research of Science, Engineering and Technology (IJIRSET)

Impact Factor 8.699

|www.ijirset.com |A Monthly, Peer Reviewed & Refereed Journal| e-ISSN: 2319-8753| p-ISSN: 2347-6710|

Volume 14, Issue 4, April 2025

|DOI: 10.15680/IJIRSET.2025.1404285|

radiation lobes compared to the main lobe. This information is crucial for understanding the antenna's radiation characteristics, including its directionality and gain, at the specified frequency of 24.5 GHz

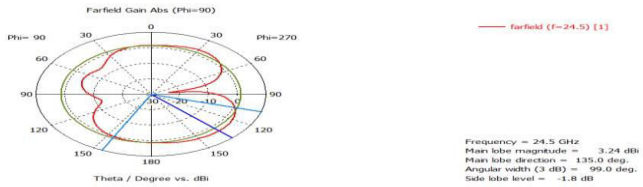

Fig. 8. Antenna of other shafesFar field radiation pattern at 24.5 Ghz

E. 3D Far-Field Radiation Pattern At 31.35 Ghz

This image presents the 3D far-field radiation pattern of the antenna at a frequency of 31.35 GHz. The visualization shows the absolute gain (Abs) in dBi, with the color scale on the right indicating the gain levels. The red regions represent areas of high gain, while the blue regions indicate low gain. The 3D shape of the radiation pattern illustrates the antenna's directivity and how it radiates power in all directions. The data provided indicates a radiation efficiency (Rad. Eff.) of -1.930 dB and a total efficiency (Tot. Eff.) of -1.934 dB. The peak gain is 6.360 dB. This 3D representation is crucial for understanding the antenna's overall radiation characteristics, including its main lobe direction, beamwidth, and side lobe levels, providing a comprehensive view of its performance in three-dimensional space

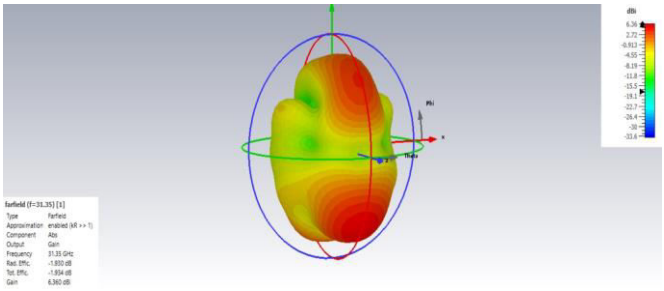

Fig. 9. 3D far-field radiation pattern at 29.375 Ghz

F. 3D far-field radiation pattern at 24.5 Ghz

This image displays the 3D far-field radiation pattern of the antenna at a frequency of 24.5 GHz. The visualization shows the absolute gain (Abs) in dBi, with the color scale on the right indicating the gain levels. The red regions represent areas of high gain, while the blue regions indicate low gain. The 3D shape of the radiation pattern illustrates the antenna's directivity and how it radiates power in all directions. The data provided indicates a radiation efficiency (Rad. Eff.) of -0.9899 dB and a total efficiency (Tot. Eff.) of -1.079 dB. The peak gain is 3.573 dB. This 3D representation is crucial for understanding the antenna's overall radiation characteristics, including its main lobe direction, beamwidth, and side lobe levels, providing a comprehensive view of its performance in three-dimensional space

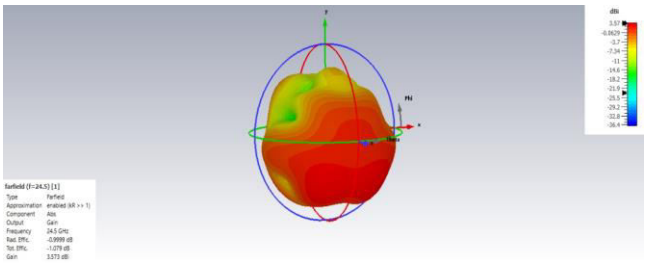

Fig. 10. 3D far-field radiation pattern at 24.5 Ghz

International Journal of Innovative Research of Science, Engineering and Technology (IJIRSET)

Impact Factor 8.699

|www.ijirset.com |A Monthly, Peer Reviewed & Refereed Journal| e-ISSN: 2319-8753| p-ISSN: 2347-6710|

Volume 14, Issue 4, April 2025

|DOI: 10.15680/IJIRSET.2025.1404285|

G. 3D far-field radiation pattern at 10.0 Ghz

This image presents the 3D far-field radiation pattern of the antenna at a frequency of 10.00 GHz. The visualization shows the absolute gain (Abs) in dBi, with the color scale on the right indicating the gain levels. The red regions represent areas of high gain, while the blue regions indicate low gain. The 3D shape of the radiation pattern illustrates the antenna's directivity and how it radiates power in all directions. The data provided indicates a radiation efficiency (Rad. Eff.) of -1.445 dB and a total efficiency (Tot. Eff.) of -1.454 dB. The peak gain is 4.546 dBi. This 3D representation is crucial for understanding the antenna's overall radiation characteristics, including its main lobe direction, beamwidth, and side lobe levels, providing a comprehensive view of its performance in three-dimensional space.

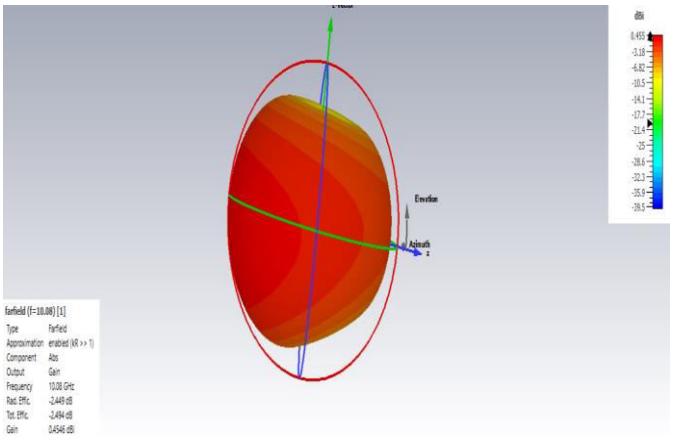

Fig. 11. 3D far-field radiation pattern at 10.0Ghz

To visualize the antenna's spatial radiation, 3D far-field gain plots were analyzed at 10 GHz, 24.5 GHz, and 31.35 GHz.

TABLE VI. 3 D RDIATION PATTERN FREQUENCIES

Frequency (GHz)	Peak Gain (dBi)	Radiation Efficiency (dB)	Total Efficiency (dB)
10.00	4.546	–1.445	–1.454
24.50	3.573	–0.990	–1.079
31.35	6.360	–1.930	–1.934

The 3D plots show dominant radiation along specific spatial lobes with color gradients indicating gain strength. Red regions signify high gain while blue regions indicate minimal radiation. The increase in gain with frequency, while maintaining acceptable efficiency, confirms the antenna's effectiveness for high-frequency applications such as mmWave 5G and beyond

V. CONCLUSION AND FUTURE SCOPE

In this paper, a compact and high-performance 2×2 MIMO microstrip patch antenna has been designed and analyzed for 5G and future 6G communication systems. The proposed antenna integrates a novel geometry with multiple feed configurations and a Y-shaped radiating patch to support wideband operation and enhanced radiation characteristics. Simulated results demonstrate multiple well-defined resonant frequencies ranging from 10 GHz to over 50 GHz, with S11 values below –10 dB across several bands. The far-field radiation patterns confirm directional radiation with acceptable beamwidths and gains up to 6.36 dBi. The influence of feedline width on impedance matching was also investigated, revealing optimal matching for wf = 0.55 mm. Furthermore, the 3D radiation plots affirm the antenna's suitability for high-gain, multi-frequency operation in mmWave and THz ranges. The antenna's compact form factor, broad frequency coverage, and satisfactory gain and efficiency make it a strong candidate for future ultra-high-speed wireless systems, including 6G networks, satellite IoT, and wearable terahertz communications. Future work can

International Journal of Innovative Research of Science, Engineering and Technology (IJIRSET)

Impact Factor 8.699

|www.ijirset.com |A Monthly, Peer Reviewed & Refereed Journal| e-ISSN: 2319-8753| p-ISSN: 2347-6710|

Volume 14, Issue 4, April 2025

|DOI: 10.15680/IJIRSET.2025.1404285|

explore the following directions to further enhance and extend the proposed design can be fabricated on a suitable high-frequency substrate to validate simulated results through physical prototyping and experimental testing.

REFERENCES

1. M. R. I. Faruque, M. T. Islam, and N. Misran, "A compact single layer dual-band microstrip patch antenna for 5G applications," *Scientific Reports*, vol. 15, no. 1, Mar. 2025.
2. A. I. Omi et al., "A new analytically designed UWB microstrip patch antenna for future 5G and 6G applications," in *2023 United States National Committee of URSI National Radio Science Meeting (USNC-URSI NRSM)*, Boulder, CO, USA, Jan. 2023, pp. 62–63.
3. M. Alibakhshikenari et al., "A comprehensive survey of metamaterial transmission-line based antennas: Design, challenges, and applications," *IEEE Access*, vol. 8, pp. 144778–144808, 2020.
4. S. Mathivanan and A. Rajeswari, "Omnidirectional microstrip MIMO antenna for 5G applications," in *2022 45th International Conference on Telecommunications and Signal Processing (TSP)*, 2022, pp. 27–30.
5. R. Ghatak, S. R. Bera, and D. R. Poddar, "A compact UWB MIMO antenna with improved isolation using defected ground structure," *IEEE Antennas Wireless Propag. Lett.*, vol. 16, pp. 1631–1634, 2017.
6. H. L. Zhu et al., "Design of a compact MIMO antenna for 5G mobile terminals," *IEEE Access*, vol. 6, pp. 52916–52924, 2018.
7. F. A. Tahir, H. Bin Zulkifli, and M. R. Kamarudin, "A review of MIMO antennas for 5G millimeter wave communications," *International Journal of Antennas and Propagation*, vol. 2018, Art. no. 5629260, 2018.
8. K. L. Wong, C. Y. Tsai, and Z. W. Liu, "5G NR sub-6 GHz metal-frame smartphone antenna array," *IEEE Access*, vol. 7, pp. 81758–81770, 2019.
9. J. Yuan et al., "A dual-band MIMO antenna array with high isolation for 5G smartphones," *IEEE Access*, vol. 7, pp. 104553–104561, 2019.
10. R. H. Khokhar and M. R. Kamarudin, "Reconfigurable antennas for 5G and beyond: A review," *Electronics*, vol. 10, no. 3, p. 327, 2021.
11. M. A. Antoniades and G. V. Eleftheriades, "A compact multiband antenna using complementary split-ring resonators (CSRR)," *IEEE Antennas Wireless Propag. Lett.*, vol. 7, pp. 652–655, 2008.
12. P. K. Singh and A. K. Gautam, "Design and analysis of CSRR-based compact multiband microstrip patch antenna," *Progress In Electromagnetics Research M*, vol. 83, pp. 55–66, 2019.
13. Y. Liu, J. Gao, and X. X. Yang, "Compact MIMO antenna system for 5G mobile terminals with high isolation and wide bandwidth," *IEEE Access*, vol. 7, pp. 127500–127510, 2019.
14. S. Wu, T. S. Rappaport, and C. M. Collins, "The human body and millimeter-wave wireless communication systems: Interactions and implications,"in *IEEE International Conference on Communications (ICC)*, 2015, pp.1–6.
15. A. I. Omi et al., "A new analytically designed UWB microstrip patch antenna for future 5G and 6G applications," in *2023 United States National Committee of URSI National Radio Science Meeting (USNC-URSI NRSM)*, Boulder, CO, USA, Jan. 2023, pp. 62–63.
16. U. Nissanov et al., "High gain terahertz microstrip array antenna for future generation cellular communication," in *2020 International Conference on Artificial Intelligence, Big Data, Computing and Data Communication Systems (icABCD)*, Durban, South Africa, 2020, pp. 1–6.
17. R. Vadlamudi and D. Sriram Kumar, "Design of a THz antenna with broadband radiation characteristics for 6G applications," in *2023 IEEE Wireless Antenna and Microwave Symposium (WAMS)*, Gandhinagar, India, 2023
18. W. A. Khan and A. Bin Muhammad, "Design and analysis of wideband THz micro size patch antenna for 6G application," in *2022 6th International Conference on Millimeter-Wave and Terahertz Technologies (MMWaTT)*, Tehran, Iran, 2022, pp. 1–4.
19. R. Yadav et al., "Ultra wideband MIMO antenna for 6G communication systems," in *2023 IEEE International Symposium on Antennas and Propagation (ISAP)*, 2023.
20. H. Aliakbarian et al., "Impact of 5G on antenna design: A review of current and future antenna trends," *IEEE Antennas Propag. Mag.*, vol. 63, no. 4, pp. 74–86, Aug. 2021

.

INTERNATIONAL STANDARD SERIAL NUMBER INDIA

INNO SPACE SJIF Scientific Journal Impact Factor

doi cross ref

निस्केयर NISCAIR

INTERNATIONAL JOURNAL OF INNOVATIVE RESEARCH

IN SCIENCE | ENGINEERING | TECHNOLOGY

9940 572 462 6381 907 438 ijirset@gmail.com

www.ijirset.com

Scan to save the contact details